Modelling Of The Ladle Furnace Preheating With A Graphite Heating Rod

Sergey Semenov[1], Patrick Namy[1], Magnus Sievers[2], Bernd Friedrich[2], John Fors[3], Krister Engvoll[3]
1. SIMTEC, Grenoble, France.
2. IME Process Metallurgy and Metal Recycling, RWTH Aachen University, Aachen, Germany.
3. Elkem Technology, Kristiansand, Norway.

Abstract
This work, which is done in the framework of the SisAl Pilot EU project, presents the use of COMSOL Multiphysics® for simulating ladle furnace preheating. The SisAl Pilot project aims at optimising the silicon production in Europe by recycling materials and using a carbon-emission friendly technology. The silicon production experiments are conducted on laboratory and pilot scales in different types of furnaces, including ladle furnaces. Besides experimental work, the process optimisation also relies on the numerical modelling. The present model simulates the preheating of an existing ladle furnace with a graphite heating rod used as a resistive element powered by a DC electric current. The aim of the work is to tune unknown problem parameters, especially graphite properties, by fitting experimental temperature curves. The adjusted material properties will be further used in the SisAl Pilot project for the numerical analysis of new ladle furnace designs. In general, the graphite properties, such as density, heat capacity, thermal and electrical conductivity, are functions of temperature and can vary depending on the material type and supplier. In the present study, we assume that the heating rod graphite and the crucible graphite differ from each other only by their porosity. With this assumption, a single set of temperature-dependent graphite properties, found in literature, can be generalised by modulating it with the material's porosity according to a preferred analytical model (Landauer's relation in this work). This makes porosity a single tuning parameter for each type of graphite in the model. The experimentally measured electric current through the heating rod serves as a known model input parameter. Measured electric power and temperatures are used for the model tuning and validation. The following COMSOL® modules are employed in this model: Heat Transfer in Solids and Fluids with convectively enhanced gas conductivity, Surface-to-Surface Radiation, and Electric Currents to simulate the Joule effect in electrically conducting materials. A bidirectional coupling of all the modules is present due to multiple interdependencies via material properties. The proposed numerical model has successfully simulated the ladle furnace preheating. The work is validated against experimental data: the tuning of model and material parameters has resulted in a satisfactory fitting of experimental curves. The adjusted graphite properties are ready to be exploited in the next stage of the SisAl Pilot project, which is focussed on the numerical analysis of new furnace designs. The presented approach of tuning material properties can be applied to other problems dealing with porous materials.

Keywords: Furnace preheating, Graphite heating rod, Radiant heat transfer.

1. Introduction
This work is done in the framework of the SisAl Pilot EU project, which is focussed on demonstrating the possibility of metallurgical grade silicon production at pilot scale based on aluminothermic reduction of silica. In comparison with the traditional carbothermic reduction of silica, the advantage of the proposed technology is in its low CO2 emission. As part of the project, the numerical modelling support of experimental works is stipulated. Development of a numerical model of ladle furnace preheating and its validation against experimental data makes possible predictive simulations and an efficient development and testing of new furnace designs. The present work is focussed on modelling of preheating of an existing ladle furnace with a graphite heating rod used as a resistive element powered by a DC electric current. The aim of the work is to tune unknown model parameters, especially graphite properties, to improve the model's predictive ability.

In section 2, experimental and numerical methods are described. Sections 3 and 4 present governing equation and material properties. In section 5, numerical results are presented. Section 6 discusses the results and compares them with experimental data. Section 7 presents the conclusions of the work.

2. Experimental and numerical methods
2.1. Experimental methods
The experiments are performed at Elkem facilities in a ladle furnace that consists of a graphite crucible, Carbon Black (Thermax® N991) refractory and steel shell, see Figure 1. The two graphite lances are used for temperature measurements and for the inert gas injection to protect the crucible from oxidation. The positions of thermocouples 102, 103, and 104 are shown in Figure 1: 102 is in a graphite lance (not shown), 103 is pressed 5 mm into the graphite crucible wall, and 104 is welded to outside steel shell. The furnace is preheated with one central graphite heating rod powered by a DC electric current with an output power of 20-24 kW.

The furnace preheating stage takes approximately 12.5 hours. The goal is to preheat crucible up to 1600 °C to get it ready for further experiments on

aluminothermic reduction of silica. During the preheating stage, the experimentally measured electric current through the heating rod serves as a known model input parameter. Measured electric power and thermocouple temperatures are used for the model tuning and validation. The power is assumed to be dissipated partially in the graphite heating rod, and partially in metal wires connected to the heating rod.
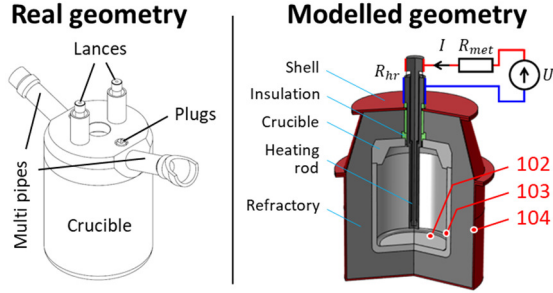

Figure 1. Real and modelled furnace geometry. R_{met} is the metal wires resistance, R_{hr} is the heating rod resistance, U is the measured voltage. Thermocouples 102, 103, 104 are indicated.

2.2. Numerical methods

To reduce problem dimensionality, an assumption of axial symmetry is made, see model geometry in Figure 1: graphite lances, plugs and multi pipes are not modelled. The numerical model is developed within COMSOL Multiphysics® software, version 6.0, which is based on the finite element method. The following COMSOL® modules are employed in this model: Heat Transfer in Solids and Fluids with convectively enhanced gas conductivity, Surface-to-Surface Radiation, and Electric Currents to simulate the Joule effect in electrically conducting materials. A bidirectional coupling of all the modules is present due to multiple interdependencies via material properties. The heat losses towards outside include an empirical boundary condition for the external natural convection in the surrounding air, heat conduction towards water cooled metal conductors connected to the heating rod, and thermal radiation towards ambient environment. Heat loss due to inert protective gas purging through an empty crucible is also considered. The experimentally measured electric current I is approximated and imposed as model input data, see Figure 2.
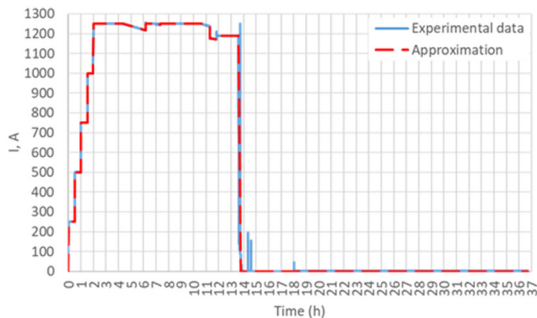

Figure 2. Electric current I through the heating rod.

The computational domain is spatially discretized with a quadrilateral mesh, as shown in Figure 3. Quadratic Lagrange elements are used in the Heat Transfer and Electric Currents modules. Linear elements are used in the Surface-to-Surface module. All computations are performed on a laptop with 8 physical cores Intel processor and 64 GB RAM.
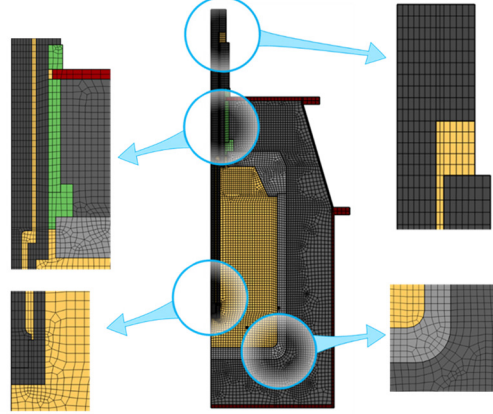

Figure 3. Computational domain discretized with a quadrilateral mesh.

3. Governing Equations

3.1. Heat transfer

In present model, the conductive heat transport is modelled in both solids and fluids. Although the convective heat transport is also present in fluids, it is not modelled directly, but replaced with an empirical model of convectively enhanced conduction. Thus, the following heat transport equation is solved in all domains:

$$\rho c_p \frac{\partial T}{\partial t} + \nabla \cdot \boldsymbol{q} = Q$$

where ρ is material density, c_p is specific isobaric heat capacity, T is temperature, t is time, Q is volumetric heat source due to Joule effect, and **q** is the conductive heat flux that also includes the convectively enhanced conduction in fluids:

$$\mathbf{q} = -\text{Nu} \cdot k \nabla T$$

where k is the thermal conductivity of materials and Nu is the Nusselt number, which equals 1 in solid materials, while in fluids it is computed according to an empirical model of convective heat transport.

On all internal interfaces that do not participate in a radiant heat exchange a condition of temperature continuity and heat flux continuity is imposed:

$$T_{up} = T_{down}$$
$$\mathbf{q}_{up} \cdot \mathbf{n} - \mathbf{q}_{down} \cdot \mathbf{n} = 0$$

where **n** is the unit normal vector at the interface, and indices "up" and "down" denote materials on two sides of the interface: "up" in direction of **n** and "down" in the opposite direction. On all external boundaries the condition of convective heat flux is imposed:

$$-\mathbf{n} \cdot \mathbf{q} = h(T_{amb} - T)$$

where **n** is the outward unit normal vector, T_{amb} is the ambient temperature, and h is the heat transfer coefficient computed according to an empirical model of external natural convection. On interfaces

and boundaries that participate in the radiant heat exchange, an additional heat source q_r is imposed due to thermal radiation absorption:

$$\mathbf{q}_{up} \cdot \mathbf{n} - \mathbf{q}_{down} \cdot \mathbf{n} = q_r$$
$$-\mathbf{n} \cdot \mathbf{q} = h(T_{amb} - T) + q_r$$

The initial furnace temperature equals the ambient one:

$$T|_{t=0} = T_{amb}$$

3.2. Surface-to-surface radiation

In the problem of surface-to-surface radiant heat exchange, the fluids (gas in crucible and gas in heating rod) are transparent, while solids are opaque to thermal radiation. The "hemicube" method is used to compute surfaces' view factors, their irradiance G_{rad} (radiant flux in W/m^2 received by a surface per unit area) and radiosity J_{rad} (radiant flux in W/m^2 leaving a surface per unit area). Before computing radiant heat fluxes in a 2D axisymmetric problem, the hemicube method reconstructs a 3D geometry by revolving the axisymmetric geometry around the axis of symmetry. For simplicity, all semi-reflecting surfaces that participate in a radiative heat exchange are assumed to give only a diffuse reflection, specular reflection is not modelled in this work. The irradiance G_{rad} of surfaces that participate in the radiant heat exchange comprises the mutual contribution G_{rad}^{mut} that comes from other surfaces or other parts of the same surface and the ambient contribution G_{rad}^{amb} that comes from the ambient environment at temperature T_{amb}:

$$G_{rad} = G_{rad}^{mut} + G_{rad}^{amb}$$
$$G_{rad}^{amb} = F_{amb}\varepsilon_{amb}n^2\sigma_{SB}T_{amb}^4$$

where F_{amb} is the ambient environment view factor, ε_{amb} is the hemispherical emissivity of the ambient environment, n is the medium refractive index ($n \approx 1$), and $\sigma_{SB} = 5.670374 \times 10^{-8}\ \text{W} \cdot \text{m}^{-2} \cdot \text{K}^{-4}$ is the Stefan-Boltzmann constant. The surface radiosity J_{rad} consists of the emitted and reflected parts:

$$J_{rad} = \varepsilon n^2\sigma_{SB}T^4 + (1-\varepsilon)G_{rad}$$

where ε is the hemispherical emissivity of the radiating surface. Thus, each surface that participates in the radiant heat exchange has the following heat source:

$$q_r = G_{rad} - J_{rad} = \varepsilon(G_{rad} - n^2\sigma_{SB}T^4)$$

3.3. Electric current

A steady-state current conservation equation is solved in the heating rod volume:

$$\nabla \cdot \mathbf{J} = 0$$
$$\mathbf{J} = \sigma\mathbf{E}, \qquad \mathbf{E} = -\nabla V$$

where $\mathbf{J}$ is the electric current density, σ is the electrical conductivity, $\mathbf{E}$ is the electric field, and V is the electric potential. The Joule effect heat source:

$$Q = \mathbf{E} \cdot \mathbf{J}$$

Boundary condition of zero electric potential $V = 0$ is imposed on one of the heating rod terminals. The experimentally measure total current I is imposed on the second heating rod terminal:

$$\int_{\partial\Omega} \mathbf{J} \cdot \mathbf{n}\, dS = I$$

4. Material properties

In general, the graphite properties, such as density, heat capacity, thermal and electrical conductivity, are functions of temperature and can vary depending on the material type and supplier. In the present study, we assume that the heating rod graphite and the crucible graphite differ from each other only by their porosity, including both open and closed pores. With this assumption, a single set of temperature-dependent graphite properties, found in literature [1, 2], can be generalised by modulating it with the material's porosity according to a preferred analytical model. The Landauer's relation, based on the effective medium percolation theory [3], is used in this work to define thermal and electrical conductivity of graphite as functions of its porosity. This makes porosity a single tuning parameter for each type of graphite in the model.

Thermal conductivity of the Carbon Black (Thermax® N991) refractory is measured as function of its density and temperature, see Figure 4.
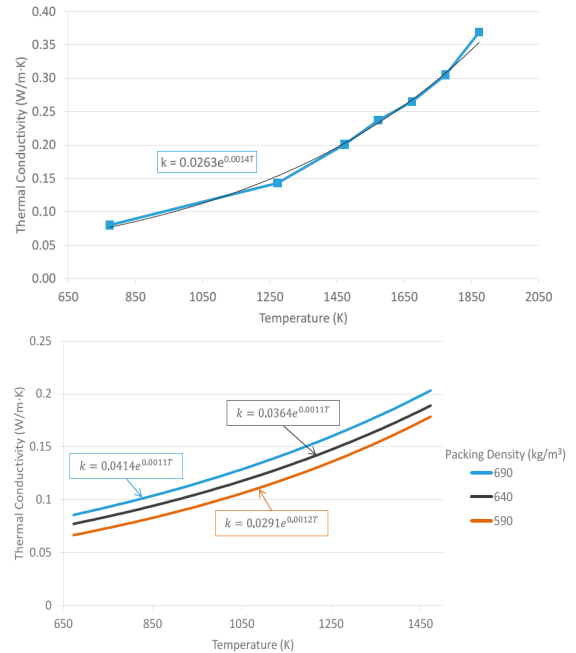

Figure 4. Thermal conductivity of Carbon Black.

5. Numerical results

The results of numerical simulations depend on several unknown model parameters, such as:

- porosity of the heating rod graphite,
- porosity of the crucible graphite,
- adjusting parameter for the thermal conductivity of Carbon Black,
- thermal conductivity of the insulation material between the heating rod and the rest of the furnace, and
- heat transfer coefficient on the heating rod terminals.

These five model parameters are iteratively adjusted to fit experimental data: to match the thermocouple temperatures and to have a Joule effect power in the heating rod, which is below the experimentally

measured one, because part of the power is lost in the out-of-furnace electrical equipment.

The following values of adjustable parameters are found to be optimal for the fitting of experimental data: porosity of the heating rod graphite is 8%, porosity of the crucible graphite is 0%, adjusting parameter of the thermal conductivity of Carbon Black is 1.35 (35% more conductive than that at the top of Figure 4), thermal conductivity of the insulation material is 100 W/m/K, and the heat transfer coefficient on the heating rod terminals is infinite, i.e. ambient temperature is imposed on the terminals.

Figure 5. Simulated temperature field in the ladle furnace.

Figure 5 demonstrates the computed temperature field in the ladle furnace after 13 hours of preheating. The maximum temperature in the ladle furnace reaches 2018 °C. This maximum is located inside of the heating rod.
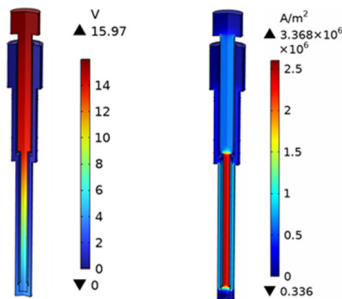

Figure 6. Simulated electric potential and electric current density in the heating rod at t = 13 h.
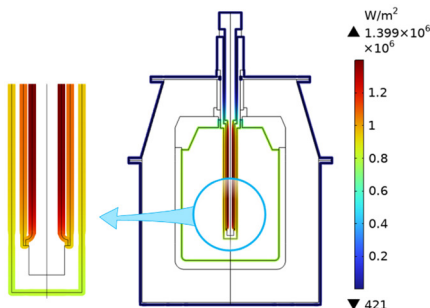

Figure 7. Surface radiosity after 13 hours of preheating.

Figure 6 shows the computed electric potential and the electric current density after 13 hours of furnace preheating. Their values directly depend on the input electric current, see Figure 2, and on the electrical conductivity of the heating rod, which is a function of temperature. At time 10.6 h the current density

reaches its maximum value of 3.54 MA/m^2, while the voltage across the heating rod reaches 16.55 V. The maximum surface radiosity of 1.4 MW/m^2 is found on the internal surface of the heating rod at the end of the preheating stage, see Figure 7.

6. Discussion, comparison with experimental data

The comparison of numerically computed temperature with thermocouple readings shows a satisfactory agreement between the model and the experiment. Figure 8 shows the comparison of numerical and experimental temperatures at the position of thermocouple 103, which is located on the internal surface of the crucible. As one can see, the initial and final temperatures are in a very good agreement. However, there is a deviation in the middle of the curve: the numerical temperature is higher than the experimental one by around 200 degrees. The possible explanation for this is that the thermocouple is in the shadow of one of the graphite lances located between the heating rod and the crucible, whereas numerical model does not include the lances.
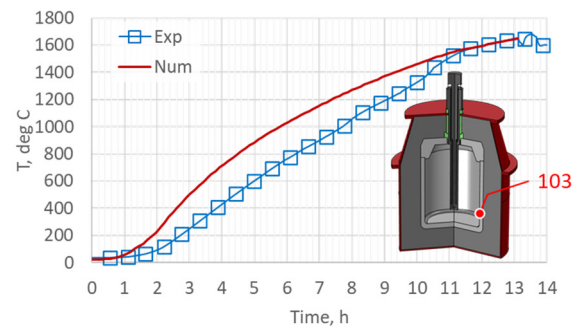

Figure 8. Numerical and experimental temperatures at the position of thermocouple 103.
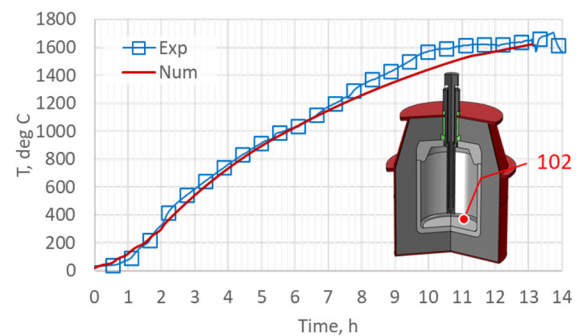

Figure 9. Numerical and experimental temperatures at the position of thermocouple 102.

As a result, the model overestimates the thermal radiation that arrives to crucible surface and therefore shows higher temperature of the crucible surface. Figure 9 shows the comparison of numerical and experimental temperatures at the position of thermocouple 102, located in one of the two graphite lances. A very good agreement between the curves is observed from the beginning up to 8 hours of the process. At around 10 hours the experimental

temperature is higher than the numerical one by around 200 degrees. As before, this could be explained by the presence of graphite lances in the experiment. This results in an additional heat source on the lances surface due to absorption of the heating rod radiation, which is not the case in the numerical model. Therefore, higher experimental temperature at the location 102 is expected and was indeed observed.

Figure 10 shows the comparison of numerical and experimental temperatures at the position of thermocouple 104, which is located on the outside surface of the steel shell. The curves show a very good agreement between the model and the experiment. The fact that from 3 to 10 hours of the process the experimental temperature is higher than the numerical one by around 5 degrees can be explained by the presence of additional external heat sources, related to auxiliary equipment, such as electrically heated metal cables, cooling systems or other furnaces used for the charge melting before pouring it into the studied furnace.
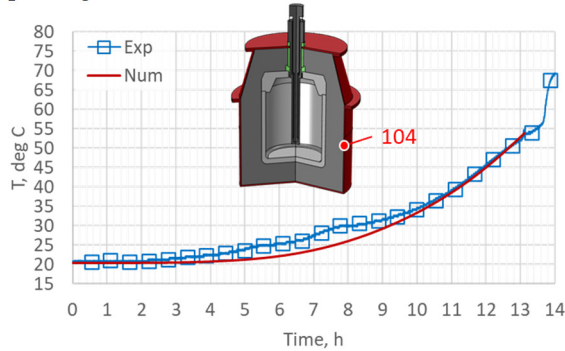

Figure 10. Numerical and experimental temperatures at the position of thermocouple 104.
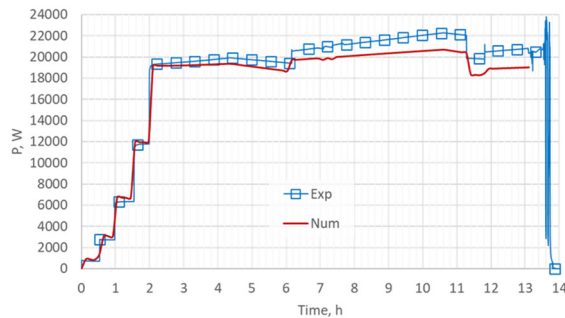

Figure 11. Numerically computed and experimentally measured electrical power dissipation.

As expected, the numerically computed power, dissipated in the heating rod, is equal to or lower than the experimentally measured one, because part of the experimental power is dissipated outside of the furnace in an external electrical equipment, see Figure 11. From the figure one can see that the power loss in the external equipment increases with time and constitutes around 8% at the end of the preheating stage.

7. Conclusions

The proposed numerical model has successfully simulated the ladle furnace preheating. The work is validated against experimental data: the tuning of model and material parameters has resulted in a satisfactory fitting of experimental curves. The adjusted graphite properties are ready to be exploited in the next stage of the SisAl Pilot project, which is focussed on the numerical analysis of new furnace designs. The presented approach of tuning material properties can be applied to other problems dealing with porous materials.

References

[1] Entegris, Inc., *Properties and Characteristics of graphite, for the semiconductor industry.,* 2013.

[2] D. McEligot, W. D. Swank, D. L. Cottle and F. I. Valentin, *Thermal properties of G-348 graphite,* Idaho Falls, ID (United States): Idaho National Lab. (INL), 2016.

[3] D. S. Smith, A. Alzina, J. Bourret, B. Nait-Ali, F. Pennec, N. Tessier-Doyen, K. Otsu, H. Matsubara, P. Elser and U. T. Gonzenbach, "Thermal conductivity of porous materials," *Journal of Materials Research,* vol. 28, no. 17, pp. 2260-2272, 2013.

Acknowledgements